

Invited Review

Two-photon excitation of fluorescence for three-dimensional optical imaging of biological structures

Alberto Diaspro*, Mauro Robello

INFN and Department of Physics, University of Genoa, via Dodecaneso 33, I-16146 Genoa, Italy

Received 15 December 1999; accepted 12 February 2000

Abstract

Techniques based on two-photon excitation (TPE) allow three-dimensional (3D) imaging in highly localized volumes, of the order of magnitude of a fraction of a femtolitre up to single-molecule detection. In TPE microscopy a fundamental advantage over conventional widefield or confocal 3D fluorescence microscopy is given by the use of infrared (IR) instead of ultraviolet (UV) radiation to excite those fluorophores requiring UV excitation, hence causing little damage to the specimen or to fluorescent molecules outside the volume of the TPE event and allowing a deeper penetration within the sample compared with conventional one-photon excitation of fluorescence. In our laboratory, within the framework of a national INFN project, we have realized a TPE fluorescence microscope, part of a multipurpose architecture also including lifetime imaging and fluorescence correlation spectroscopy modules. The core of the architecture is a mode-locked Ti:sapphire infrared pulsed laser pumped by a high-power (5 W, 532 nm) solid-state laser and coupled to an ultracompact scanning head. For the source we have measured a pulse width from 65 to 95 fs as function of wavelength (690–830 nm). The scanning head allows conventional and two-photon confocal imaging. Point spread function measurements are reported with examples of applications to the study of biological systems. ©2000 Elsevier Science S.A. All rights reserved.

Keywords: Two-photon excitation; 3D Microscopy; Biostructures; Fluorescence imaging

1. Introduction

Two-photon excitation (TPE) fluorescence microscopy is a comparatively new form of far-field fluorescence optical microscopy with advantages over both widefield and confocal laser scanning microscopy (CLSM) for the study of the three-dimensional (3D) and dynamic properties of biological systems [1–8]. One of the major unfavourable conditions occurring in 3D widefield and confocal schemes is that the whole specimen is harmed by fluorescence excitation within an hourglass-shaped region [9–12]. This fact produces the negative effect that a lot of potentially interesting biological experiments are defeated by photobleaching of the fluorescent label and phototoxicity, especially when there is the need for 3D imaging coupled with the use of UV-excitabile fluorochromes [2,5]. The advent of TPE laser scanning microscopy alleviates these concerns, opening new perspectives to the application of microscopic techniques to the study of

biological systems and related phenomena and providing further attractive advantages over classical 3D microscopy [1,3,5].

The story dates back to 1931 when the Nobel laureate Maria Goppert Mayer predicted the phenomenon of two-photon absorption as a single quantum transition in her doctoral dissertation [13,14]. Around 1961, thanks to the availability of laser sources, Kaiser and Garret reported TPE in $\text{CaF}_2:\text{Eu}^{2+}$ [15]. Later, Rentzepis et al. produced photographs of the three-photon excited fluorescence in organic dye [16]. In 1974 Hellwarth and Christensen exploited optical non-linearity for second-harmonic generation in ZnSe polycrystals at microscopic level [17]. It was the Oxford group led by Sheppard and Wilson that outlined how such a non-linear optical phenomenon could be exploited in microscopy when combined with the evolving scanning optical microscope [18–20]. Jumping to the 1990s, the work done by Denk et al. at the W.W. Webb laboratories (Cornell University, Ithaca, NY) revolutionized fluorescence microscopy imaging [1]. They demonstrated that this non-linear effect, combined with the sharp focusing of a microscope objective

* Corresponding author. Tel.: +39-10-3536426; fax: +39-10-314218; e-mail: diaspro@fisica.unige.it

lens, produces an inherent optical sectioning or 3D effect. Two-photon excitation rapidly evolved to different related techniques like fluorescence correlation spectroscopy, lifetime imaging, real-time TPE, third-harmonic generation, 4PI two-photon microscopy, 3D tracking, single molecule detection, two-photon-excited flash photolysis, flow cytometry, TPE active devices and so on [4,7,8,21,22].

2. Two-photon excitation of fluorescent molecules

Conventional 3D microscopy, both computational wide-field and confocal, suffers from the drawback that photobleaching and phototoxicity strongly affect the biological systems throughout the whole volume confining the fluorescence excitation. This situation is dramatically alleviated in the case of TPE, which allows the excitation volume to be minimized and utilizes low-energy wavelengths. In fact, due to the physics of the process, fluorophore excitation occurs by simultaneous absorption of two photons, which co-operatively provide the energy needed to prime the fluorescence process. The energies of two photons can combine only if these photons interact with the same fluorophore at the *same* time. The time interval for *simultaneity* is the time scale of molecular energy fluctuations at photon energy scales, as determined by the Heisenberg uncertainty principle, i.e., 10^{-16} s [14]. These two photons do not necessarily have to be identical. What it is relevant is that their wavelengths, λ_A and λ_B , are such that

$$\lambda_1 \cong \left(\frac{1}{\lambda_A} + \frac{1}{\lambda_B} \right)^{-1} \quad (1)$$

where λ_1 is the wavelength needed to prime fluorescence emission at a wavelength λ_2 in conventional or one-photon mode, as sketched in Fig. 1 using a Jablonski-like diagram.

The TPE process requires high photon flux densities on the order of 10^{31} photons/cm²·s. This situation of high instantaneous photon flux density can be obtained by tight focusing of a laser beam. So far in a TPE process it is crucial to combine sharp spatial focusing with temporal confinement of the excitation beam. It has been demonstrated that for a train of beam pulses focused through a high-numerical-aperture (NA) objective, for a duration τ_p with repetition rate f_p , the probability, n_a , that a certain fluorophore simultaneously absorbs two photons during a single pulse, in the paraxial approximation, is ruled by the following relationship [1]:

$$n_a \propto \frac{\delta_2 P_{ave}^2}{\tau_p f_p^2} \left(\frac{NA^2}{2\hbar c \lambda} \right)^2 \quad (2)$$

where δ_2 is the two-photon cross section of the fluorescent molecule, P_{ave} the time-averaged power of the beam and λ the excitation wavelength.

For a δ_2 of approximately 10^{-58} [m⁴·s] per photon, focusing through an objective of high NA = 1.2–1.4, an average incident laser power of ≈ 30 –50 mW, operating at a wave-

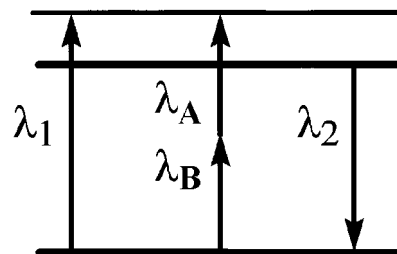


Fig. 1. Simplified Jablonski-like diagram sketching the excitation process in one- and two-photon absorption. A general situation is depicted according to Eq. (1).

length ranging from 640 to 1000 nm with 100 fs pulsewidth and 100 MHz repetition rate, would saturate the fluorescence output at the limit of one photon pair per pulse per fluorophore [1]. Table 1 reports conditions related to energy delivery in the case of one- and two-photon excitation cases. Recently, the cross-section parameter has been measured for a wide range of dyes [23,24]. Table 2 summarizes the excitation properties of some common fluorescent molecules. The main problem is that knowledge of one-photon cross sections does not permit any quantitative prediction of two-photon ones. As a ‘rule of thumb’, especially in symmetrical rather than in complex molecules, one may expect to have the cross-section peak at double the wavelength with respect to one-photon

Table 1

	Two photon	One photon
Excitation rate	$N_2 \propto \delta l_e^2$	$N_1 \propto \sigma l_e$
Cross section	$\delta_2 \sim 10^{-50}$ cm ⁴ s/photon	$\sigma_1 = 10^{-16}$ cm ²
Laser	$P_e \sim 100$ mW mode-locked $\tau_p \sim 100$ fs $f_p \sim 100$ MHz $P_{max} \sim P_e$ $\tau_p f_p \sim 104 P_e$	$P_e \sim 1$ mW continuous $P_{max} = P_e$
Focusing 1 mm laser beam to 1 μ m spot at specimen	$I_e \sim 100$ mW/ mm ² $I_{e,max} \sim 10^5$ W/ μ m ²	$I_e \sim 1$ mW/ cm ²

Table 2

Dyes	Excitation/Emission wavelengths (nm)	Two-photon cross section (cm ⁴ s/photon)
Indol-1 free	700/490	3.5×10^{-50}
Indo-1 Ca ²⁺	700/405	1.5×10^{-50}
DAPI	700/450	0.16×10^{-50}
Coumarin 307	776/530	1×10^{-49}
Fluorescein	782/520	1×10^{-48}
Rhodamine B	840/600	2×10^{-48}
Lucifer Yellow	860/533	1×10^{-50}
Fura-2 free	700/510	11×10^{-50}
Fura-2 Ca ²⁺	700/510	12×10^{-50}

excitation conditions. It is worth noting that, also due to the increasing dissemination of TPE microscopy, new ‘ad hoc’ organic molecules, endowed with large two-photon absorption cross sections, have recently been developed [25].

Another aspect reported through Eq. (2) is that, due to the characteristics of the optical focalization [26], the excitation power falls off as the square of the distance from the point of focus, within the approximation of a conical illumination geometry. This means that the quadratic relationship between the excitation power and the fluorescence intensity brings out the fact that TPE falls off as the fourth power of distance from the point of focus of the objective being used. This fact implies that those regions away from the focal volume of the objective lens, directly connected to the numerical aperture of the objective itself, will therefore not suffer photobleaching or phototoxicity effects when TPE is used. They are simply not involved in the excitation process. A confocal-like effect is obtained without the necessity of a confocal pinhole [27,28]. Fig. 2 depicts the situation from the perspective of the specimen. In TPE over 80% of the total fluorescence intensity comes from a 700–1000 nm thick region about the focal point for objectives with numerical apertures in the range from 1.2 to 1.4. This also implies a dramatic reduction of background that allows the reduction in spatial resolution due to the larger diffraction-limited spot with respect to the conventional case where half the wavelength is used to be compensated [28,30]. The utilization of infrared instead of UV–visible wavelengths is also responsible for deeper imaging than in the conventional case [29].

3. A TPE architecture for 3D imaging

Nowadays, there are two popular approaches to realizing TPE imaging architectures [4,8,31–34]. The first approach uses exactly the same optical pathway and mechanism as in CLSM. Pinholes are removed or set to their maximum aperture and the emission signal is captured using galvanometric scanning mirrors. This is called the descanned mode. The other approach is called the non-descanned mode. In non-descanned mode, the CLSM optical path is modified in order to increase the signal-to-noise ratio and pinholes are removed. The emitted radiation is collected using dichroic mirrors on the emission path or external detectors without passing through the galvanometric scanning mirrors. In order to obtain a better spatial resolution, it is also possible to keep the confocal pinholes. Unfortunately, in some practical experimental situations, the low efficiency of the TPE fluorescence process may rule out such a solution. However, when pinhole insertion is possible, the major advantage is attained in terms of axial resolution, which can be ameliorated by approximately 40% [27,30,35].

3.1. A descanned TPE architecture

In our laboratory, within the strategic framework of a national project of the National Institute of the Physics of

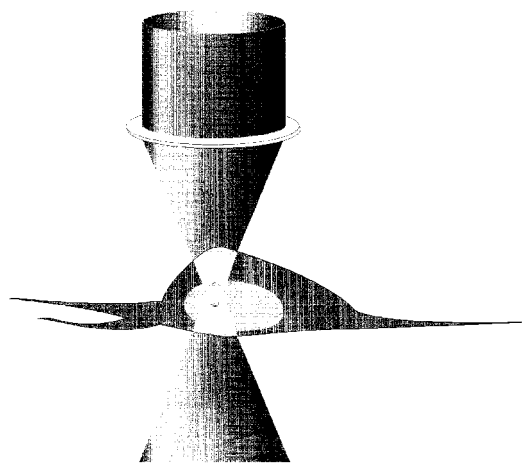


Fig. 2. The excitation phenomenon takes place only within a diffraction-limited volume of event. This volume of event, the bright ellipsoid in the centre of the excitation volume, can be roughly quantified using the resolution parameters of the system.

Matter (INFM), we have realized a TPE fluorescence microscope, part of a multipurpose architecture also including lifetime imaging and fluorescence correlation spectroscopy modules [6,32]. The architecture of the TPE microscope is outlined in Fig. 3. The core of the architecture is a mode-locked Ti:sapphire infrared pulsed laser (Tsunami 3960, Spectra Physics, Mountain View, CA, USA), pumped by a high-power (5 W at 532 nm) solid-state laser (Millennia V, Spectra Physics). The features of the infrared pulsed laser are high average power, 80 MHz repetition rate, and 100 fs pulse width. High peak power is critical for efficient photon excitation and consequently average power, and is related to it by the duty cycle D according to

$$P_{\text{ave}} \approx DP_{\text{peak}} \quad (3)$$

$$D = \tau_p f_p \quad (4)$$

The use of short pulses and small duty cycles is mandatory to allow image acquisition in a reasonable time while using power levels that are biologically tolerable [5,34,37].

The laser beam is directly coupled to the scanning head. Our choice is related to the fact that the whole system is still growing and we need maximum flexibility and minimum level of ‘extra’ problems at this stage. At present there are some problems related to a fibre-coupling solution. Some research groups are working on it and a commercial system is available, but some drawbacks still remain. In fact, due to high-order non linearities in the fibre, not much power can be put through it (60–100 mW). Moreover, because the fibre coupler needs some devices for maintaining pulse width and beam shape, it is not totally turnkey, demanding for further control and alignment procedures especially when wavelength changes are required. We do not perform any measurement of the pulse width at the sample, which requires a delicate and complex procedure [31,35,36], assuming that at the focal volume a 1.5–2 times broadening occurs when using a high-numerical-aperture objective [35]. In our case, i.e., for a measured laser pulse width of about 80 fs [32], the

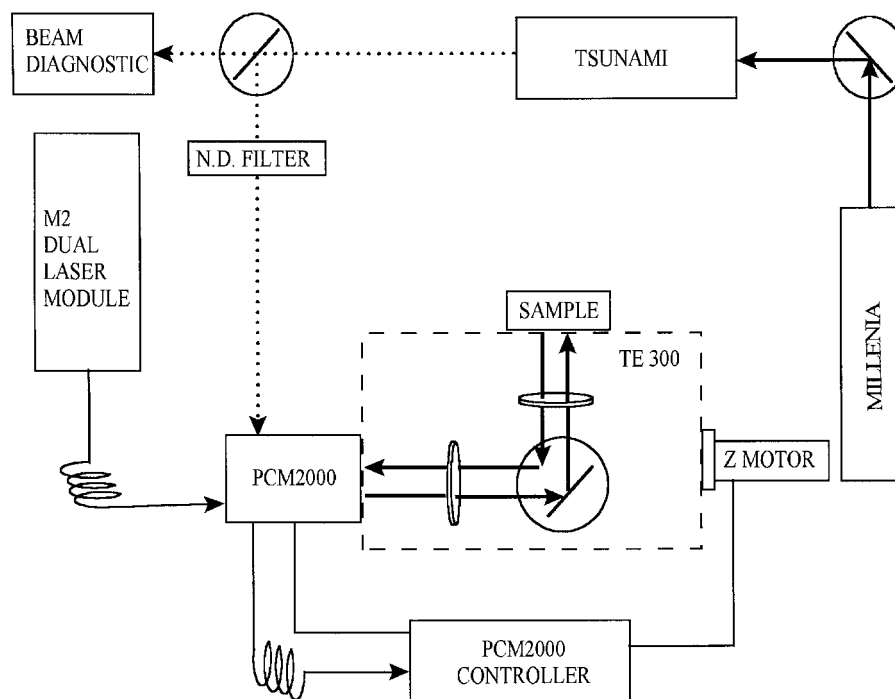


Fig. 3. Architecture of the TPE microscope operating as a national facility of the National Institute of the Physics of Matter. Schematic drawing of the TPE confocal laser scanning microscope using the single-pinhole PCM2000 scanning head coupled to conventional and pulsed laser sources. Beam diagnostics are performed using an ultrafast laser spectrum analyser (RE201, Ist-Rees, UK) and a thermopile detector power meter (AN2/10A-P, Ophir, Israel). The M2 dual laser module is the excitation module for conventional excitation; it contains two laser sources, argon ion and He–Ne, providing 488 and 543 nm excitation wavelengths, respectively. The M2 module is connected through an optical fibre to the scanning head, which allows a fast switching to two-photon excitation by simply disconnecting the optical fibre and allowing direct coupling of the IR pulsed beam.

estimate at the sample is about 150 fs in the more favourable situation.

The scanning and acquisition system for microscopic imaging is based on a commercial scanning head (Nikon PCM2000, Nikon Instruments, Florence, Italy) mounted on the lateral port of a Nikon Eclipse TE300 inverted microscope. The scanning head operates in the ‘open pinhole’ condition; i.e., a wide-field descanned detection scheme is used. A planachromatic Nikon 100 \times , 1.4 NA immersion oil objective has been used. The optical resolution performance of this scanning head when operating in confocal and TPE mode has been reported elsewhere [32,38]. One-photon and two-photon modes can be simply accomplished by switching from a mono-mode optical fibre (one-photon) coupled to conventional laser sources to an optical path in air guiding the IR laser beam (two-photon). The same entrance port of the scanning head is used and in both cases, an optical fibre delivers the emitted fluorescence to the PCM2000 control unit where photomultiplier tubes (R928, Hamamatsu, Japan) are physically plugged in. A dichroic mirror (Chroma, Brattleboro, VT, USA) has been substituted in the original scanning head to allow excitation from 680 to 1050 nm and the neutral-density filter at the open-pinhole location has been removed. Moreover, a series of custom-made emission filters, which block infrared radiation (> 650 nm) to an optical density of 6–7 within 50 mW of beam power incident on the filters themselves, have been utilized, namely: E650P, HQ 460/50, HQ 535/50, HQ 485/30 and HQ 405/30 (Chroma).

Axial scanning is actuated by means of two different positioning devices, namely, a belt-driven system using a d.c. motor (RFZ-A, Nikon, Japan) and a single-objective piezo nano-positioner (PIFOC P-721-17, Physik Instrument, Germany).

Acquisition and visualization are completely computer controlled by EZ2000 dedicated software (Coord, The Netherlands).

The images shown in this paper have been acquired using a 720 nm laser beam operating at 80 fs pulse width and 80 MHz repetition rate as evaluated at the laser output window. The laser power has been reduced by variable neutral-density filters (CVI, CT, USA) to an average value of 20 mW at the entrance of the scanning head. The average power before the microscope objective is about 9–13 mW and at the sample it is estimated to be between 3 and 5 mW [2].

3.2. Point spread function behaviour

To characterize the spatial resolution of the TPE system, blue fluorescent carboxylate modified microspheres 0.1 μm in diameter (F-8797, Molecular Probes, OR, USA) were used. A drop of dilute samples of bead suspensions was spread on a coverslip of nominal thickness 0.17 mm and air dried in a dust-clean chamber. These microspheres constitute a very good compromise regarding the utilization of sub-resolution point scatterers and acceptable fluorescence emission given the expected resolution of TPE. An object plane

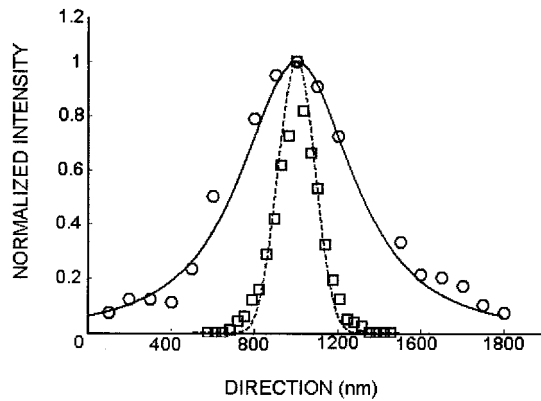


Fig. 4. The experimentally determined radial (square) and axial (circle) intensity profiles and the corresponding theoretical point spread functions (solid line for the axial, dotted line for the radial). The quadratic dependence on the excitation intensity, which forms the basis for the application of TPE for 3D microscopy, has been checked for a solution of fluorescein (Merck, Germany) in water. All intensity data, corrected only for background and measured in the central subarea of the scanned region, fell within a logarithmic best-fit straight line with a slope of 1.9996 ($R=0.9965$).

field of $18 \mu\text{m} \times 18 \mu\text{m}$ was imaged in a 512×512 frame, at a pixel dwell time of $17 \mu\text{s}$.

We imaged 21 z -sections of fluorescent beads with z -scan steps of 100 nm . The x - y scan step was 35 nm . The PCM2000 pinhole was set to the open position. The 3D data sets of 10 microspheres were analysed. The measured full width at half

maximum (FWHM) lateral and axial resolutions were 210 and 700 nm , respectively. These results are in agreement with the prediction of the Fraunhofer diffraction approximation. Experimental data and theoretical expectations are reported in Fig. 4. For the same scanning head, operating in confocal condition and one-photon excitation mode, the experimental lateral and axial FWHM resolution parameters were evaluated as 180 and 500 nm , respectively [38].

3.3. Imaging of UV-excitabile fluorescent molecules and optical sectioning

Fig. 5 shows images of rat granule cerebellar cultured cells loaded with Fura-2, a calcium-specific marker with excitation in the UV region. Fig. 6 shows 3D frames from the optical sections.

Another example of TPE imaging is given in the study of the structure of sperm heads of the Octopus *Eledone cirrhosa*. The sample has been prepared according to a previously published procedure [39]. We used a UV-excitabile fluorescent dye, i.e., DAPI (4',6-diamidino-2-phenylindole hydrochloride), to visualize the helical structure in a 3D framework [24].

Fig. 7 shows a 3D representation of the helical structure realized by assembling 2D images from a stack of 64,

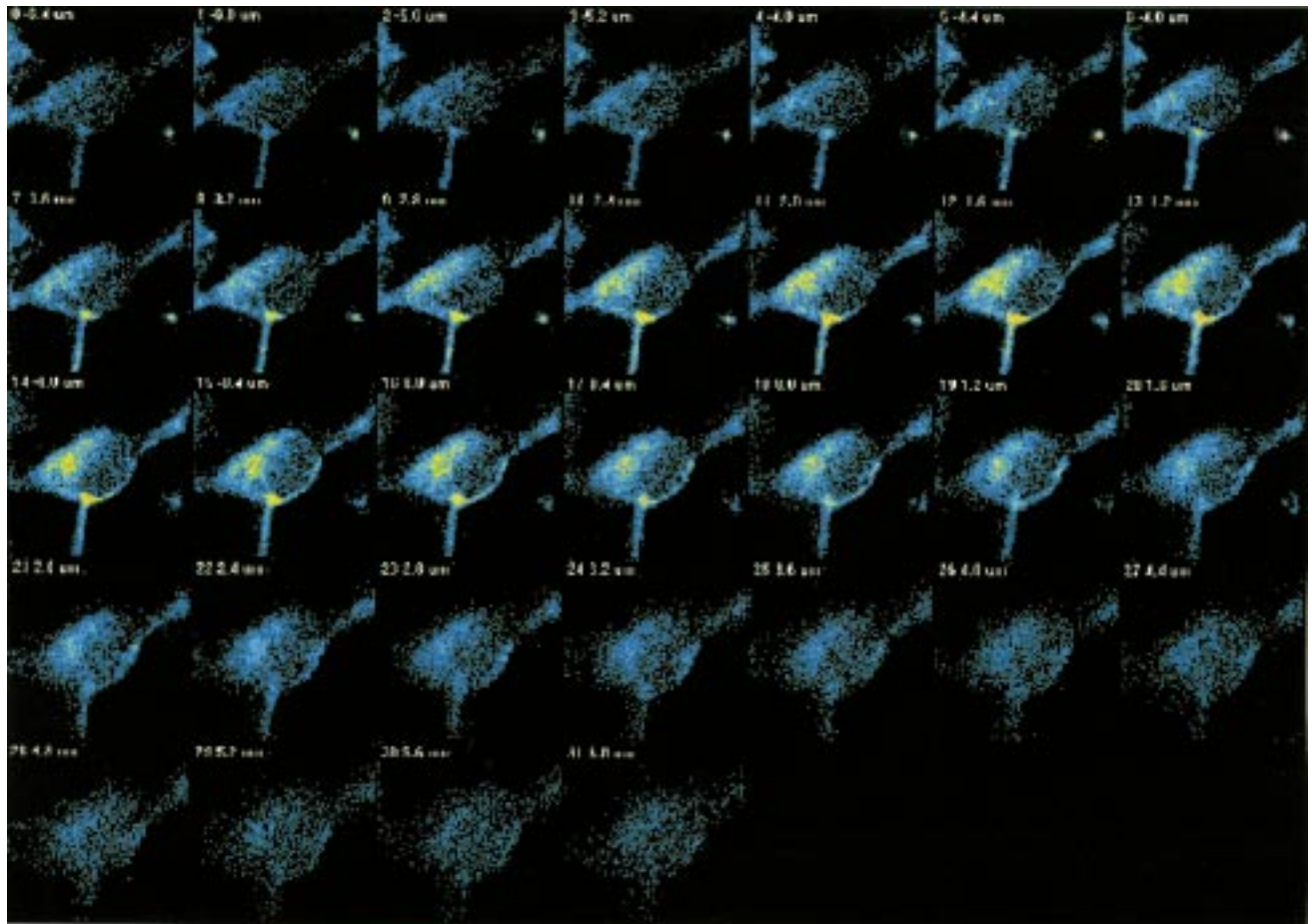


Fig. 5. An example of TPE optical sections obtained from rat granule cerebellar cells loaded with Fura2.

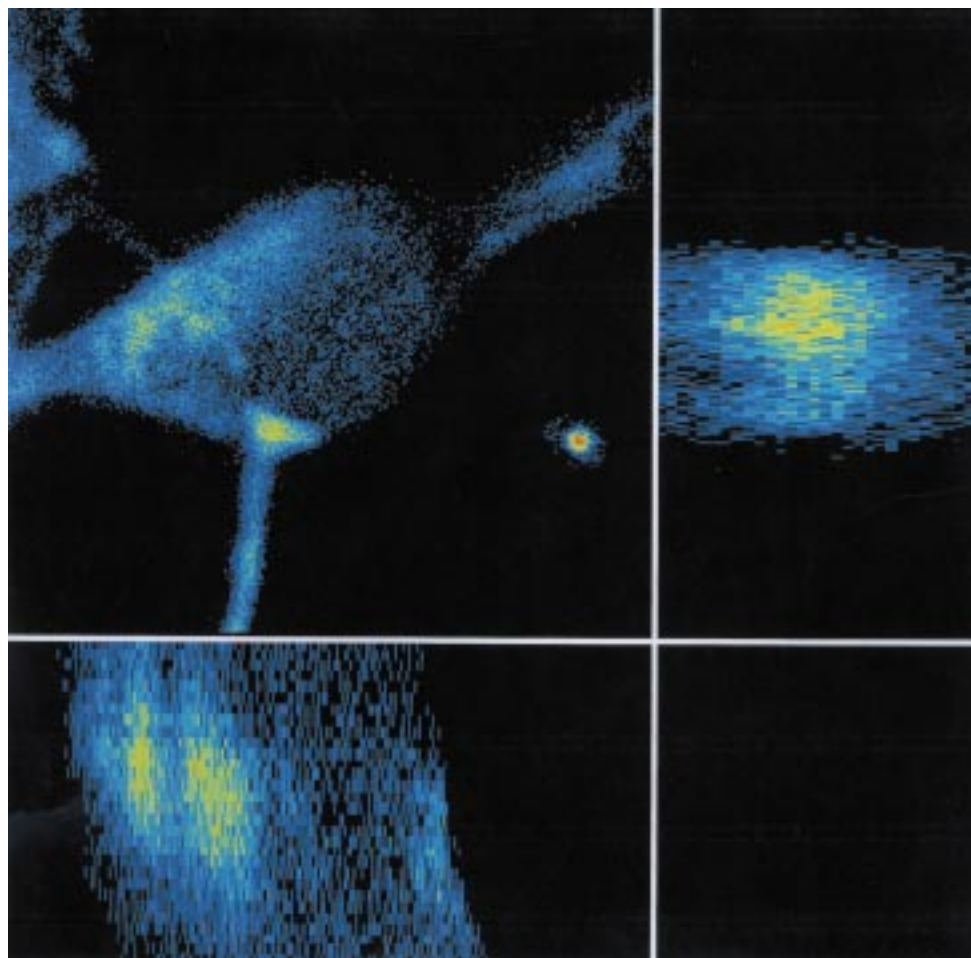


Fig. 6. Following Fig. 5, image sections assembled in a 3D frame: x - y (centre), y - z (right) and x - z (bottom) views.

512 × 512 × 8 bits, taken 200 nm apart along the optical axis. The dimensions of the sperm head are pitch = 0.6–0.75 μm, outer radius = 0.25–0.3 μm and length = 43 μm. From the collection of 2D images it is not possible to get information about the spatial organization of the sperm head. As in the case of 3D optical sectioning performed using conventional confocal microscopy [39], the handedness can be determined only by using the complete set of 2D slices.

The TPE microscope has also been used with a wide range of other fluorescent molecules like Indo-1, Oregon Green, Rhodamine, DiOC₆(3), fluorescein and Texas Red (data not shown). These dyes are normally excited in a single-photon range from UV to green.

4. Conclusions

TPE microscopy broke into the arena bringing its intrinsic 3D resolution, the absence of background fluorescence, and the charming possibility of exciting UV-excitable fluorescent molecules at infrared wavelengths, increasing sample penetration. Photobleaching is considerably reduced since the infrared pulsed laser light excitation occurs only at the focal plane, and multiple excitation of fluorescent molecules can

be more easily and efficiently accomplished than in conventional excitation. The situation also changes for problems related to autofluorescence, but this topic is too complex and needs a more detailed analysis [22,34,40]. Two-photon excitation microscopy is becoming an essential imaging system for thick-sample and live-cell imaging.

Under a fluorescence acquisition perspective, ballistic and scattered emitted photons can be allowed to contribute to the total acquired signal: they have been uniquely produced in a very specific volume. What is invaluable for cell imaging, and in particular for live-cell imaging, is the fact that the weak endogenous absorption and highly localized spatial confinement of the TPE process dramatically reduce phototoxicity stress. Some studies are oriented to elucidate the possible induced photodamage and irreversible sample modification due to the use of high laser intensities [36,37,41–44]. To the best of our knowledge, the situation is still advantageous if compared with the damage induced by means of conventional fluorescence excitation. Notwithstanding this, some sagacity has to be used and some experimental parameters need to be tightly controlled, such as power, dwell time and pulse width [41].

Recent outstanding applications have been experienced in the study of impurities affecting the growth of protein crystals

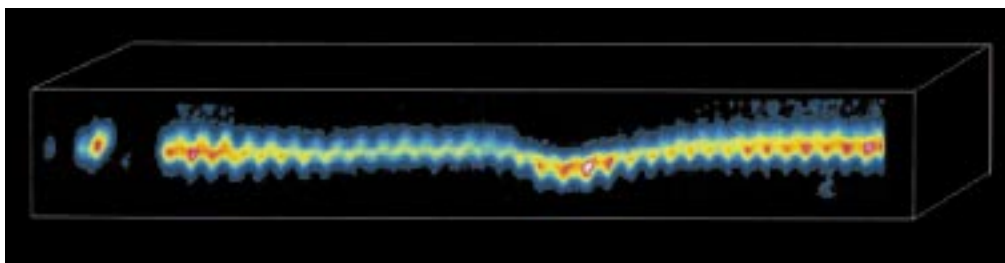


Fig. 7. The 3D assembly of the mature sperm head of the Octopus *Eledone cirrhosa*, loaded with DAPI, visualized in a 3D fashion from 12 optical slices.

[45] and in fluorescence imaging of samples marked with green fluorescent protein (GFP) [46]. Moreover, a single-molecule detection by TPE of fluorescence was carried out on fluorescein, measuring the diffusion of less than two molecules in the probe volume, and on rhodamine, performing measurements in a flowing cell [47]. Another important field of application is the utilization of the TPE microscope architecture for microscopic polymerization [48]. It is also worth noting the use of the TPE microscope architecture for spectroscopic and lifetime studies [21,49,50].

In order to summarize some of the advantages of TPE, we recall the following further aspects:

1. Repeated scanning on the specimen in confocal microscopy, particularly with UV light, induces rapid photoisomerization and high background autofluorescence. TPE microscopy reduces these complications, providing better penetration at infrared wavelengths and thus prolonging cell viability during image acquisition.
2. The conventional excitation technique requires special UV optics for the UV excitation probe, while TPE uses conventional microscope optics.
3. In one-photon excitation, the emission wavelength is close to the excitation wavelength (about 50–200 nm). In TPE, the fluorescence emission occurs at a wavelength substantially shorter than the excitation wavelength.

At present, the main disadvantage of TPE fluorescence microscopy is the cost of femtosecond laser sources. As also pointed out by other researchers, once technology becomes less expensive and simpler, there will not be a confocal, or a light, microscope that is not also a two-photon microscope.

5. Queries for authors

Refs. [42,48]: please supply names of **all** authors. Table 1: what does l_c stand for?

Acknowledgements

This work is supported by INFM grants.

References

- [1] W. Denk, J.H. Strickler, W.W. Webb, Two-photon laser scanning fluorescence microscopy, *Science* 248 (1990) 73–76.
- [2] J.B. Pawley (Ed.), *Handbook of Biological Confocal Microscopy*, Plenum Press, New York, 1995.
- [3] S.M. Potter, Vital imaging: two photons are better than one, *Current Biol.* 6 (1996) 1596–1598.
- [4] S.W. Hell, Nonlinear optical microscopy, *Bioimaging* 4 (1996) 121–123.
- [5] D.W. Piston, Imaging living cells and tissues by two-photon excitation microscopy, *Trends Cell Biol.* 9 (1999) 66–69.
- [6] A. Diaspro, M. Robello, Multi-photon excitation microscopy to study biosystems, *Microsc. Anal.* 58 (1999) 5–7.
- [7] A. Diaspro (Guest Ed.), Two-photon microscopy, *Microsc. Res. Tech.* 47 (1999) 163–212.
- [8] A. Diaspro (Guest Ed.), Two-photon excitation microscopy, *IEEE Eng. Med. Biol. Mag.* 18 (5) (1999) 16–99.
- [9] D.A. Agard, Optical sectioning microscopy: cellular architecture in three dimensions, *Annu. Rev. Biophys.* 13 (1984) 191–219.
- [10] T. Wilson, C.J.R. Sheppard, *Theory and Practice of Scanning Optical Microscopy*, Academic Press, London, 1984.
- [11] B. Bianco, A. Diaspro, Analysis of the three dimensional cell imaging obtained with optical microscopy techniques based on defocusing, *Cell Biophys.* 15 (1989) 189–200.
- [12] T. Wilson (Ed.), *Confocal Microscopy*. Academic Press, London, 1990.
- [13] M. Göppert-Mayer, Über Elementarakte mit zwei Quantensprüngen, *Ann. Phys.* 9 (1931) 273–295.
- [14] O. Nakamura, Fundamentals of two-photon microscopy, *Microsc. Res. Tech.* 47 (1999) 165–171.
- [15] W. Kaiser, C.G.B. Garret, Two-photon excitation in $\text{CaF}_2:\text{Eu}^{2+}$, *Phys. Rev. Lett.* 7 (1961) 229–231.
- [16] P.M. Rentzepis, C.J. Mitschle, A.C. Saxman, Measurement of ultrashort laser pulses by three-photon fluorescence, *Appl. Phys. Lett.* 17 (1970) 122–124.
- [17] R. Hellwarth, P. Christensen, Nonlinear optical microscopic examination of structures in polycrystalline ZnSe, *Opt. Commun.* 12 (1974) 318–322.
- [18] J.N. Gannaway, C.J.R. Sheppard, Second harmonic imaging in the scanning optical microscope, *Opt. Quant. Electron.* 10 (1978) 435–439.
- [19] C.J.R. Sheppard, R. Kompfner, Resonant scanning optical microscope, *Appl. Optics* 17 (1978) 2879–2885.
- [20] T. Wilson, C.J.R. Sheppard, Imaging and super resolution in the harmonic microscope, *Opt. Acta* 26 (1979) 761–770.
- [21] P.T.C. So, K.M. Berland, T. French, C.Y. Dong, E. Gratton, Two photon fluorescence microscopy: time resolved and intensity imaging, in: X.F. Wang, B. Herman (Eds.), *Fluorescence Imaging Spectroscopy and Microscopy*, Chemical Analysis Series, vol. 137, Wiley, New York, 1996, pp. 351–373.
- [22] P. Schwille, U. Haupts, S. Maiti, W.W. Webb, Molecular dynamics in living cells observed by fluorescence correlation spectroscopy with one- and two-photon excitation, *Biophys. J.* 77 (1999) 2251–2265.
- [23] C. Xu, W.W. Webb, Measurement of two-photon excitation cross-sections of molecular fluorophores with data from 690 nm to 1050 nm, *J. Opt. Soc. Am. B* 13 (1996) 481–491.
- [24] I. Gryczynski, H. Malak, J.R. Lakowicz, Multiphoton excitation of the DNA stains DAPI and Hoechst, *Bioimaging* 4 (1996) 138–148.

- [25] M. Albota, et al., Design of organic molecules with large two-photon absorption cross sections, *Science* 281 (1998) 16153–16156.
- [26] M. Born, E. Wolf, *Principles of Optics*, 6th ed., Pergamon, Oxford, 1993.
- [27] M. Gu, C.J.R. Sheppard, Effects of a finite sized pinhole on 3D image formation in confocal two-photon fluorescence microscopy, *J. Mod. Opt.* 40 (1993) 2009–2024.
- [28] M.B. Cannell, C. Soeller, High resolution imaging using confocal and two-photon molecular excitation microscopy, *Proc. R. Microsc. Soc.* 32 (1997) 3–8.
- [29] V.E. Centonze, J.G. White, Multiphoton excitation provides optical sections from deeper within scattering specimens than confocal imaging, *Biophys. J.* 75 (1998) 2015–2024.
- [30] O. Nakamura, Three-dimensional imaging characteristics of laser scan fluorescence microscopy: two-photon excitation vs. single-photon excitation, *Optik* 93 (1993) 39–42.
- [31] C. Soeller, M.B. Cannell, Construction of a two-photon microscope and optimisation of illumination pulse duration, *Pflugers Arch.* 432 (1996) 555–561.
- [32] A. Diaspro, M. Corosu, P. Ramoino, M. Robello, Adapting a compact confocal microscope system to a two-photon excitation fluorescence imaging architecture, *Microsc. Res. Tech.* 47 (1999) 196–205.
- [33] A. Periasamy, P. Skoglund, C. Noakes, R. Keller, An evaluation of two-photon excitation versus confocal and digital deconvolution fluorescence microscopy imaging in *Xenopus morphogenesis*, *Microsc. Res. Tech.* 47 (1999) 172–181.
- [34] W. Denk, D. Piston, W.W. Webb, Two-photon molecular excitation in laser scanning microscopy, in: J. Pawley (Ed.), *Handbook of Biological Confocal Microscopy*, Plenum Press, New York, 1995, pp. 445–458.
- [35] P.E. Hanninen, S.W. Hell, Femtosecond pulse broadening in the focal region of a two-photon fluorescence microscope, *Bioimaging* 2 (1994) 117–121.
- [36] M. Muller, J. Squier, G.J. Brakenhoff, Measurements of femtosecond pulses in the focal point of a high numerical aperture lens by two-photon absorption, *Optics Lett.* 20 (1995) 1038–1040.
- [37] A. Schonle, S.W. Hell, Heating by absorption in the focus of an objective lens, *Optics Lett.* 23 (1998) 325–327.
- [38] A. Diaspro, S. Annunziata, M. Raimondo, M. Robello, Three-dimensional optical behaviour of a confocal microscope with single illumination and detection pinhole through imaging of subresolution beads, *Microsc. Res. Tech.* 45 (1999) 130–131.
- [39] A. Diaspro, F. Beltrame, M. Fato, A. Palmeri, P. Ramoino, Studies on the structure of sperm heads of *Eledone cirrhosa* by means of CLSM linked to bioimage-oriented devices, *Microsc. Res. Tech.* 36 (1997) 159–164.
- [40] J.D. Bhawalkar, et al., Two-photon laser scanning fluorescence microscopy from a fluorophore and specimen perspective, *Bioimaging* 4 (1996) 168–178.
- [41] H.J. Koester, D. Baur, R. Uhl, S.W. Hell, Ca^{2+} fluorescence imaging with pico- and femtosecond two-photon excitation: signal and photodamage, *Biophys. J.* 77 (1999) 2226–2236.
- [42] C.J. Bardeen, et al., Effect of pulse shape on the efficiency of multiphoton process, *J. Biomed. Optics* 4 (3) (1999) 362–367.
- [43] K. Konig, P.T.C. So, W.W. Mantulin, E. Gratton, Cellular response to near-red femtosecond laser pulses in two-photon microscopes, *Opt. Lett.* 22 (1997) 135–136.
- [44] K. Konig, T.W. Becker, P. Fischer, I. Riemann, K.J. Halbhauer, Pulse-length dependence of cellular response to intense near-infrared laser pulses in multiphoton microscopes, *Optics Lett.* 24 (1999) 113–115.
- [45] C.L. Caylor, I. Dobrianov, C. Kimmer, R.E. Thorne, W. Zipfel, W.W. Webb, Two-photon fluorescence imaging of impurity distributions in protein crystals, *Phys. Rev. E* 59 (1999) 3831–3834.
- [46] M. Chalfie, S. Kain, *Green Fluorescent Protein*, Wiley Liss, New York, 1998.
- [47] J.M. Song, T. Inouè, H. Kawazumi, T. Ogawa, Single molecule detection by laser two-photon excited fluorescence in a capillary flowing cell, *Anal. Sci.* 14 (1998) 913–915.
- [48] B.H. Cumpston, et al., Two-photon polymerization initiators for three-dimensional optical storage and microfabrication, *Nature* 348 (1999) 51–54.
- [49] J. Sytsma, J.M. Vroom, C.J. De Grauw, H.C. Gerritsen, Time-gated fluorescence lifetime imaging and microvolume spectroscopy using two-photon excitation, *J. Microsc.* 191 (1998) 39–51.
- [50] D.W. Piston, D.R. Sandison, W.W. Webb, Time resolved fluorescence imaging and background rejection by two-photon excitation in laser scanning microscopy, *Proc. SPIE* 1640 (1992) 379–389.